BEST AVAILABLE IMAGES

Defective images within this document are accurate representations of the original documents submitted by the applicant.

Defects in the images may include (but are not limited to):

- BLACK BORDERS
- TEXT CUT OFF AT TOP, BOTTOM OR SIDES
- FADED TEXT
- ILLEGIBLE TEXT
- SKEWED/SLANTED IMAGES
- COLORED PHOTOS
- BLACK OR VERY BLACK AND WHITE DARK PHOTOS
- GRAY SCALE DOCUMENTS

IMAGES ARE BEST AVAILABLE COPY.

As rescanning documents *will not* correct images, please do not report the images to the Image Problem Mailbox.

REMARKS

I. INTRODUCTORY REMARKS

The applicants respectfully request reconsideration and allowance of the application.

Upon entry of this Amendment, claims 89-130, 133-156, 158-199, 202-215, 217, and 219-290 are believed pending.

The applicants thank the Examiner for his review of a large number of claims and his allowance of selected claims. In view of the partial allowance, the applicants herein amend the claims to reduce the number of issues in this application so the case may timely proceed to issue. The applicants, however, traverse each of the rejections in the December 1, 2003 office action raised by the Examiner including in particular each of the prior art rejections based on Jaschke, Mirkin, Okada, or a combination thereof. The applicants herein are only responding to some of the rejections presented by the Examiner for some of the claims to reduce the number of issues. In not responding to other rejections, the applicants are not conceding that these other rejections are correct in any way and in no way are waiving their rights to traverse these rejections. Rather, one or more additional applications will be filed wherein these issues can be addressed.

Upon entry of the present Amendment, the claims can be classified into three groups:

I) Claims 1-87 were originally filed and subjected to restriction.

II) Claims 88-218 were filed in a Preliminary Amendment (August 8, 2003) responsive to the restriction

III) Claims 219-290 are introduced in the present Amendment. Introduction of these new claims, however, is not believed to require new searching for reasons explained below. The Examiner should contact the undersigned if new searching is believed needed.

Also, the pending claims can be organized based on the independent claims:

I) Independent Claim 90 and claims dependent thereon: 89, 91-130, 133-156;

II) Independent Claim 159 and claims dependent thereon: 158, 160-199, 202-214;

III) Independent Claim 215 and claims dependent thereon: 219-245;

IV) Independent Claim 217 and claims dependent thereon: 246-268;

V) Claims 269-290 based on allowed subject matter.

II. PATENTABILITY OF CLAIMS WHICH ARE ONLY REJECTED ON MIRKIN

In the February 10, 2004 personal interview, the applicants proposed amending the claims so that only a single prior art reference was at issue, and the Examiner favorably reviewed this approach to simplifying the issues and bringing the case to allowance.

In the December 1, 2003 Office Action, the Examiner has exclusively relied on a paper by Piner and Mirkin, "Effect of Water on Lateral Force Microscopy in Air," *Langmuir*, 1997, 13, 6864-6868 ("Mirkin") to reject the following claims: dependent claims 90, 94-96, 159, 163-165, 170, 172-177, 182, 206, and independent claims 215 and 217. Hence, these claims should be allowed if found patentable over Mirkin.

Now, the applicants demonstrate why claims 215, 217, 90, and 159 are patentable over Mirkin (upon entry of the present Amendment, all four claims are written in independent format).

A. Patentability of Independent Claim 215

> *215. A method of direct-write nanolithography comprising transporting molecules in a positive printing mode from an atomic force microscope tip to a solid substrate of interest by capillary transport, wherein the molecules have a chemical affinity for the solid substrate.*

The Examiner rejected independent claim 215 for a single reason: for being anticipated by Mirkin. The Examiner states that Mirkin teaches that the surface may be hydrophilic and that hydrophilic surfaces inherently have an affinity for water. Therefore, according to the Examiner, Mirkin teaches the claim language "*...wherein the molecules have a chemical affinity for the solid substrate.*" The applicants respectfully traverse.

Mirkin fails to teach or suggest the recited "chemical affinity." Hence, there can be no anticipation. Mirkin merely discloses that water can be transported from an AFM tip to a mica surface to form vanishing, meta-stable structures which is not consistent with and does not suggest chemical affinity.

Chemical affinity generally is understood and described in the specification to mean some type of chemical interaction, covalent reaction, or chemisorption is occurring which goes beyond a mere non-chemical affinity interaction. For example, the dictionaries and encyclopedias describe a relevant context for "chemical affinity":

> *"Chemical Affinity: The entropy production due to a chemical reaction..."* (Van Nostrand's Scientific Encyclopedia, 6th Ed., 1983; copy enclosed).

The Examiner's own cited dictionary definition of chemisorption (page 254 included with office action) is consistent with this concept and recited "formation of bonds" which are "comparable in strength to ordinary chemical bonds and much stronger than the Van der Waals type characterizing physical adsorption" and result in chemisorbed molecules being "altered."

The applicants' specification, moreover, describes the use of many molecules which have a chemical affinity for the substrate (see, for example, page 1, line 30, and extensive listing of compounds and substrates on page 13, line 5 to page 18, line 5 which provide chemisorption or

covalent bonding). The prior art, Mirkin, is also distinguished in the specification on page 3, first paragraph, and one skilled in the art would interpret claim 215 based on the specification and its characterization of Mirkin:

> *...water, depending upon relative humidity and substrate wetting properties, will either be transported from the substrate to the tip or vice versa. In the latter case, metastable, nanometer-length scale patterns could be formed from very thin layers of water deposited from the AFM tip (Piner et al.,* Langmuir, 13:6864 (1997). *The present invention shows that when the transported molecules can anchor themselves to the substrate, stable surface structures are formed resulting in a new type of nanolithography, DPN.* (emphases added)

In other words, the specification teaches that Mirkin's water deposits are only metastable which means any hydrophilic affinity between water and the mica substrate in Mirkin is not the type of chemical affinity recited for the claimed nanolithography. Mirkin itself expressly teaches that the water *vanishes*:

> *It was also observed that the deposits imaged here vanish over a period of about a day, presumably by surface diffusion.* (page 6867, right column).

This vanishing effect found in Mirkin is consistent with other prior art wherein thin films of water easily dry and disappear. For example, Hu et al., *J. Surface Science*, 344 (1995) 221-236 teaches at page 232 that "droplets were found to disappear by evaporation unless the humidity was kept at or above 56%" (copy enclosed). Hu also teaches on page 232 that "[i]t is known that after long exposure to air, mica becomes slightly hydrophobic," which further undermines the Examiner's assumption that mica is necessarily hydrophilic and that water has a chemical affinity for mica. Therefore, Mirkin does not teach or suggest chemical affinity, and the Examiner should withdraw the rejection of claim 215.

B. Patentability of Independent Claim 217

> *217. A method comprising: coating an AFM tip with an ink; bringing the coated AFM tip into contact with a substrate in the presence of a transport medium which forms a meniscus; writing with the tip.*

The Examiner has also rejected independent claim 217 for being anticipated by Mirkin. The Examiner states that, in Mirkin, the patterning compound itself forms the meniscus and, consequently, reads on the claimed transport medium. The applicants respectfully traverse.

Mirkin does not teach or suggest coating an AFM tip with an ink. Hence, there can be no anticipation. Moreover, Mirkin does not teach the recited ink which one skilled in the art would understand is functionally different than the transport medium. One skilled in the art would manifestly presume that the ink and the transport medium are given different names because they are functionally different and not the same. Ink is present apart from the transport medium. Nothing in the specification suggests otherwise. For example, claim 217 and the supporting specification expressly contemplate that the tip can be coated with the ink, apart from a transport medium. In addition, the specification teaches:

> *Suitable transport media include water, hydrocarbons (e.g., hexane), and solvents in which the patterning compounds are soluble (e.g., the solvent used for coating the tip – see above).* Page 20, lines 12-14.

Here again, the functions of the transport media and the ink are differentiated. Hence, the Examiner's interpretation of the claim, wherein the ink and the transport medium is the same, is not consistent with the specification, and one skilled in the art reading claim 217 would readily recognize that the Mirkin does not teach or suggest the subject matter of claim 217.

C. Patentability of Independent Claims 90 and 159

> *90. A direct-write nanolithographic method comprising:*
> *providing a solid substrate:*
> *providing an atomic force microscope tip having a patterning compound coated thereon; and*

delivering the patterning compound from the tip to the substrate so as to produce a stable pattern on the solid substrate, wherein the delivery step is carried out with flow of the patterning compound from the tip to the substrate by capillary action.

159. A direct-write nanolithographic method comprising:

providing a solid substrate;

providing a tip having an ink thereon; and

delivering the ink from the tip to the substrate so as to produce a stable nanostructure on the solid substrate, wherein the delivering step is carried out with flow of the ink from the tip to the substrate by capillary action.

In the present Amendment, claims 90 and 159 were rewritten in independent form to include the subject matter of the base claims (88 and 157, respectively, which are canceled).

For reasons explained above in sections IIA and IIB, claim 90 also is not anticipated by Mirkin. Mirkin only describes vanishing metastable patterns, whereas claim 90 recites stable patterns. These stable patterns can be achieved by methods not taught or suggested by Mirkin including chemical affinity, chemisorption, covalent bonding with the surface as a stabilization method. Hence, there can be no anticipation.

Similarly, for reasons explained above in sections IIA and IIB, claim 159 also is not anticipated by Mirkin. Mirkin only describes vanishing metastable patterns, whereas claim 159 recites "stable nanostructure." Mirkin does not suggest use of chemisorption, chemical affinity, covalent bonding, or other stabilization methods. Hence, there can be no anticipation.

In sum, the above four claims (215, 217, 90, and 159) are patentable over Mirkin and should be allowed together with claims dependent thereon.

III. NEWLY INTRODUCED CLAIMS

Newly introduced claims 269-290 represent allowed subject matter as they recite aspects not described by the prior art according to the Examiner in the December 1 office action. This

subject matter includes use of DNA, oligonucleotides, nucleic acids, amines, silanes, gold, and silicon (see pages 18-19 of the office action). Hence, these claims should also be allowed and should not require new searching. The Examiner should contact the undersigned by telephone if he believes otherwise.

IV. FINAL MATTERS

The applicants thank the Examiner for returning the initialized PTO-1449 forms along with the December 1, 2003 office action.

The applicants also confirm in the record that the attached patent family chart dated October 27, 2003 was submitted to the Examiner by facsimile on October 27, 2003 for his convenience which shows the patent family filing for the present application and its parent and related applications, all being handled by the Examiner apparently. An updated chart is also submitted herewith.

In particular, if the Examiner wants to discuss any interference related issues for attorney docket numbers 083847-0139 and 083847-0140, the Examiner should contact the undersigned as soon as possible. These interferences are being pursued by the applicants in view of US Patent Nos. 6,270,946 to Miller and 6,573,369 to Henderson et al, respectively. The undersigned confirms the Examiner's phone call to him on February 27, 2004 regarding the restriction requirement in the 083847-0139 matter and on March 5, 2004 regarding the status of 083847-0140. The applicants believe that the presently pending claims are entitled to a filing date of January 7, 1999 and that the applicants' priority application is dominating prior art against U.S. Patent Nos. 6,270,946 and 6,573,369. The Examiner should contact the undersigned if further discussion is needed about the interference filings and the allowance of the present case.

The applicants traverse the December 1, 2003 restriction requirement, including numerous specific opinions for supporting restriction, but have elected group I merely to reduce the number of issues.

Replacement figures 1-28B are being submitted in response to the Examiner's request for better copies.

The specification has been Currently Amended to update the priority claim.

The Examiner has rejected claim 216 for being indefinite. The applicants respectfully traverse. The applicants, however, have cancelled claim 216 to reduce the number of issues but reserve the right to prosecute the subject matter of claim 216 in one or more other applications.

The Examiner has rejected claims 37, 97, 103, 110, 116, 117, 120, 121, 166, 172, 179, 185, 186, 189, 190, 216, and 218 for double patenting. The applicants respectfully traverse, making no admission thereby about the scope of the claims at issue. The applicants have either cancelled or Currently Amended these rejected claims for now to reduce the number of issues but reserve the right to prosecute the subject matter of these claims in one or more other applications. If the Examiner continues to believe that a double patenting rejection is warranted, the Examiner should contact the undersigned to move the case to allowance.

Please find attached a check for $110.00 for the one month extension of time fee due in this application

The Commissioner is hereby authorized to charge any additional fees which may be required regarding this application under 37 CFR §§ 1.16-1.17, or credit any overpayment, to Deposit Account No. 19-0741. Should no proper payment be enclosed herewith, as by a check being in the wrong amount, unsigned, post-dated, otherwise improper or informal or even entirely missing, the Commissioner is authorized to charge the unpaid amount to Deposit Account No. 19-0741.

Respectfully submitted,

Date: March 9, 2004

By _____

FOLEY & LARDNER, LLP
Washington Harbour
3000 K Street, N.W., Suite 500
Washington, D.C. 20007-5143
Telephone: (202) 672-5569
Facsimile: (202) 672-5399

J. Steven Rutt
Attorney for Applicants
Registration No. 40,153

VAN NOSTRAND'S SCIENTIFIC ENCYCLOPEDIA

Sixth Edition

Animal Life
Biosciences
Chemistry
Earth and Atmospheric Sciences
Energy Sources and Power Techonology
Mathematics and Information Sciences
Materials and Engineering Sciences
Medicine, Anatomy, and Physiology
Physics
Plant Sciences
Space and Planetary Sciences

DOUGLAS M. CONSIDINE, P.E.
Editor

GLENN D. CONSIDINE
Managing Editor

VAN NOSTRAND REINHOLD COMPANY
NEW YORK CINCINNATI TORONTO LONDON MELBOURNE

CHELATES (Boiler Water). Feedwater (Boiler).

CHELATING AGENTS (Anemia). Anemias.

CHELICERAE. The first pair of appendages in spiders and related animals. They are associated with the mouth and are formed for chewing and in some cases for grasping, as in the scorpions.

CHELIPED. An appendage of the thorax formed for grasping, in the crustaceans. The chela or pincher of the lobster and crayfish.

CHEMICAL AFFINITY. The entropy production due to a chemical reaction has the form

$$\frac{d_i S}{dt} = \frac{1}{T} \mathbf{A} v \geq 0 \tag{1}$$

where **A** is the chemical affinity and v, the reaction rate. **A** is related to the characteristic functions U, H, A, G, and to the chemical potentials μ by the relations:

$$\begin{aligned} \mathbf{A} &= -\left(\frac{\partial U}{\partial \xi}\right)_{S.\,V} = -\left(\frac{\partial H}{\partial \xi}\right)_{S.\,p} \\ &= -\left(\frac{\partial A}{\partial \xi}\right)_{T.\,V} = -\left(\frac{\partial G}{\partial \xi}\right)_{T.\,p} \\ &= -\sum_i \nu_i \mu_i \end{aligned} \tag{2}$$

when ξ is the extent of reaction and ν_i the stoichiometric coefficient.

The basic properties of the affinity **A** are that it is always of the same sign as the reaction rate, and that if the affinity is zero the reaction rate is also zero, i.e., the system is in equilibrium.

This definition of affinity is essentially due to De Donder and is called De Donder's fundamental inequality. In the notation used by G. N. Lewis and his school, it is supposed that ξ increases by unity, therefore the relations of (2) are written in the form:

$$\mathbf{A} = -(\Delta U)_{S.V.} = -(\Delta H)_{S.p} = -(\Delta A)_{T.\,V} = -(\Delta G)_{T.\,p}. \tag{3}$$

Note that in this entry, **A** is the affinity and A, the Helmholtz function (work function).

See also **Chemical Reaction Rate.**

CHEMICAL ANALYSIS. Analysis (Chemical).

CHEMICAL CARCINOGENS. Cancer and Oncology; Carcinogens.

CHEMICAL COMPOSITION. Matter is composed of the chemical elements, which may be in the free or elementary state, or in combination. In the former case, as exemplified by iron, tin, lead, sulfur, iodine, and the rare gases, matter commonly exhibits the properties of the atoms of the particular element, including the chemical properties whereby they combine to form molecules. Molecules may (1) be monoatomic; (2) they may consist of atoms of one element only, such as nitrogen or hydrogen molecules (N_2 or H_2), (3) they may be composed of atoms of more than one element, called compounds, which usually have distinctive properties.

The molecular formulas of gaseous compounds are obtained from a study of the composition by elements and the density, by a method introduced by the Italian chemist, Cannizzaro, in 1858. Later, in 1872, in the course of his Faraday Lecture before the Chemical Society (London) on the subject "Some Points in the Teaching of Chemistry" Cannizzaro stated that "Symbols and formulas, in my opinion, constitute the introduction, preparation, and base of the study of the transformations of matter, which is the true object of our science." The simplest way to understand the method is to arrange in tabular form (1) the individual gases, (2) the weight in grams of 1 liter (at 0°C, 760 millimeters of mercury pressure) of each gas, (3) the weight in grams of *each element* present in the above volume (1 standard liter) found by exact analysis (percentage composition by chemical elements using the methods of analytical chemistry). See Table 1.

TABLE 1. CANNIZZARO METHOD OF COMPOUND COMPUTATION

Gas	Grams per Standard Liter	Percentage Composition by Chemical Elements		Grams per Standard Liter by Chemical Elements					
				Hydrogen	Oxygen	Carbon	Nitrogen	Sulfur	Chlorine
1. Hydrogen chloride	1.639	Hydrogen	2.76%	0.045					1.594
		Chlorine	97.24						
2. Ammonia	0.771	Hydrogen	17.75	0.137			0.634		
		Nitrogen	82.25						
3. Carbon dioxide	1.977	Oxygen	72.73		1.438	0.539			
		Carbon	27.27						
4. Carbon monoxide	1.250	Oxygen	57.14		0.714	9.536			
		Carbon	42.86						
5. Methane	0.717	Hydrogen	25.14	0.180		0.537			
		Carbon	74.86						
6. Ethylene	1.260	Hydrogen	14.38	0.181		1.079			
		Carbon	85.62						
7. Acetylene	1.173	Hydrogen	7.75	0.091		1.082			
		Carbon	92.25						
8. Oxygen	1.429	Oxygen	100.00		1.429				
9. Hydrogen	0.090	Hydrogen	100.00	0.090					
10. Nitrogen	1.251	Nitrogen	100.00				1.251		
11. Chlorine	3.214	Chlorine	100.00						3.214
12. Sulfur dioxide	2.927	Oxygen	49.95		1.462			1.465	
		Sulfur	50.05						
13. Hydrogen sulfide	1.539	Hydrogen	5.91	0.091				1.448	
		Sulfur	94.09						
14. Nitrous oxide	1.978	Oxygen	36.35		0.719		1.259		
		Nitrogen	63.65						
15. Nitric oxide	1.340	Oxygen	53.32		0.715		0.625		
		Nitrogen	46.68						
Minimum weight (approximate)				0.045	0.715	0.538	0.626	1.45	1.60

NOTE: Data are displayed in this table to illustrate the Cannizzaro method of arriving at the symbol and symbol weight of chemical elements; and the formula and formula weight of chemical compounds.

ELSEVIER

Surface Science 344 (1995) 221–236

surface science

The structure of molecularly thin films of water on mica in humid environments

J. Hu [1], X.-d. Xiao [2], D.F. Ogletree, M. Salmeron *

Materials Sciences Division, Lawrence Berkeley Laboratory, University of California, Berkeley, CA 94720, USA

Received 26 June 1995; accepted for publication 8 August 1995

Abstract

The structures formed by the condensation and evaporation of water on mica surfaces at room temperature have been imaged with nanometer resolution. The technique used is based on the measurement of the polarization force between a charged AFM tip and the surface. This allowed us to perform non-contact imaging at tip–surface distances of a few hundred ångströms, which is critical to not perturb the surface of liquid layers. We found that at room temperature and up to 40–50% humidity, water condenses forming two-dimensional, molecularly thin films with two distinct phases (I & II). Phase I forms at humidities <20%, while phase II forms between ~20 and 40%. Phase II forms polygonal domains in angular epitaxial relationship with the mica crystallographic directions, suggesting that it is solid in character. Above 40% humidity, water adsorbs forming thicker films and droplets.

Keywords: Atomic force microscopy; Evaporation and sublimation; Liquid surfaces; Liquid–gas interfaces; Mica; Water; Wetting

1. Introduction

The scanning tunneling and the atomic force microscopes (STM and AFM) have revolutionized the science of nanostructures by providing real space images with atomic scale resolution [1]. In addition, these techniques can operate in any environment – vacuum, gas and liquid – opening the way for atomic scale studies of surfaces and processes in many technologically important areas and in practical operating conditions. Most surfaces and interfaces have been studied in this way with the exception of the liquid–gas and liquid–liquid interfaces. These, as well as the surfaces of solids with very weakly bound adsorbates present considerable difficulties due to the perturbation caused by the tip. In the case of a liquid, due to the high mobility of its surface, the close proximity of the tip can produce perturbations in its shape and wetting under the action of capillary forces.

We have recently developed a new technique, which we called scanning polarization force microscopy (SPFM), that exploits the force due to the electrical polarization of any substrate when approached by a charged object [2]. In the SPFM, this is the biased tip of an AFM. With this technique, the imaging problems mentioned above are circumvented since the tip scans at a large enough distance (a few 100 Å) from the surface to

* Corresponding author. Fax: +1 510 486 4995; E-mail: salmeron@stm.lbl.gov.

[1] Permanent address: Shanghai Institute of Nuclear Research, Academia Sinica, P.O. Box 800-204, Shanghai 201800, People's Republic of China.

[2] Present address: Department of Physics, Hong Kong University of Science and Technology, Clear Water Bay, Kowloon, Hong Kong.

SSDI 0039-6028(95)00858-6

not perturb the liquid layers. With it, we have imaged a variety of liquid structures on many substrates that exhibit a variety of wetting and chemical reaction properties [3].

Water is the most important liquid due to its role in life chemistry, as a universal solvent, and as a geological element in rain, oceans and in the soil. Its interaction with solid surfaces is of paramount importance in chemistry, electrochemistry and biology. The surfaces of its solid and liquid phases, by themselves or when interacting with other solid and liquid surfaces, determine such important phenomena as acid rain, pollution, washing and rinsing, ice chemistry of the stratosphere, etc. Wetting phenomena are important in all aspects of science and technology and in everyday life.

This important role of water is reflected in recent publications dealing with the structure of water at interfaces using modern techniques. Non-linear optics (sum frequency generation) was used to probe the OH vibrational stretch at the free water [4] surface and at the quartz–water interface [5]. In the first case, it was found that more than 20% of the surface molecules have one free OH projecting out into the vapor phase. In the second case, dipolar orientation was established that depends on the relative strength of electrostatic and hydrogen bonding interactions at the interface. Ordering of water monolayers at the metal–solution interface was established by Porter et al. [6] using tunnel junctions between Hg droplet electrodes and by Toney et al. using grazing X-ray diffraction [7]. Many Monte Carlo and molecular dynamics simulations have been carried out also that predict ordering near the metal surface [8]. An extensive review of the water adsorption on metal surfaces has been published by Thiel and Madey [9]. In the case of mica, the presence of a water monolayer and of water layered structures leading to oscillatory forces and several adhesion minima in surface force apparatus experiments has been reported [10,11].

In the high resolution imaging area beyond the optical diffraction limit however, no studies exist that explore the structure of water or other liquids on surfaces. The SPFM technique provides a unique method to achieve nanometer resolution on liquids, opening the way for studies of water adsorption at interfaces. In this paper we present a detailed account of our study of the structures formed by the condensation and evaporation of water at room temperature on mica substrates. A brief account of these results has been published recently [12].

2. Experimental

The technique of SPFM has been described in detail elsewhere [2], therefore only a brief account is given here. The crucial element is the sharp metallized tip of an AFM that produces a strong and localized electric field when biased. Our tips were produced by coating a commercially available microfabricated cantilever (we used Digital Instrument Si_3N_4 levers with nominal 0.58 N/m spring constant), with ~20 Å of Cr followed by 100 Å of Pt. It is polarized by biasing it with a positive or negative DC voltage V of 1–10 V, or by an AC voltage of similar amplitude. For neutral surfaces, the attractive electrostatic forces due to the polarization of the sample material is proportional to V^2. For charged surfaces, the force varies as $(V_0+V)^2$, where V_0 is a constant that depends on the initial surface charge.

In front of a flat conductive substrate, a point charge q gives rise to a surface polarization charge distribution that is equivalent to an image charge $-q$. On a thick (semiinfinite) insulting substrate with dielectric constant ε, the image charge is $\{-(\varepsilon-1)/(\varepsilon+1)\}\cdot q$ (we assume the environment around the tip is air) [13]. A real tip is, of course, more complicated than a point charge and the polarization force assumes a more complicated form or must be numerically calculated. However, the basic idea is the same. A schematic of the SPFM principle is shown in Fig. 1. The sample is mounted on a piezoelectric tube scanner and the deflection of the lever under the influence of tip–surface forces is measured by the light beam reflection technique using a segmented photodiode detector. SPFM imaging is done by maintaining a constant value of the attractive polarization force by means of an electronic feedback control [14].

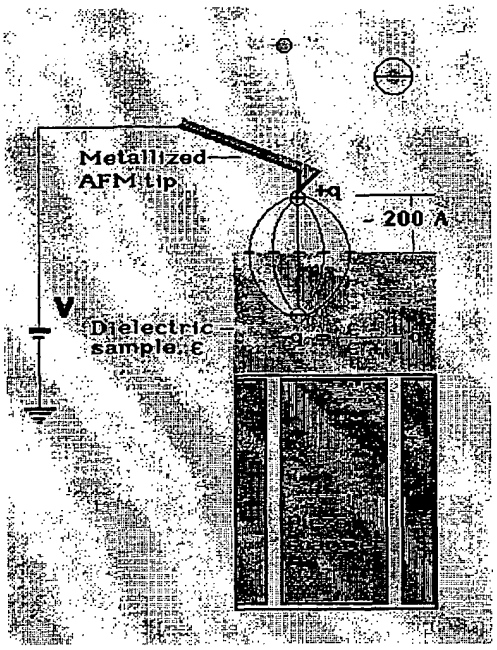

Fig. 1. Schematic drawing describing the principle of scanning polarization force microscopy (SPFM). The strong electric field from a sharp charged AFM tip polarizes any nearby substrate giving rise to an attractive electrostatic force. This force depends on the dielectric properties of the substrate. Typical operating conditions are: bias ±2–3 V, tip–surface distance 100–300 Å and net attractive force 5–10 nN.

Typical values of this force are 1–10 nN for a tip–substrate distance of 100–300 Å.

The AFM head is enclosed in a plastic box. The relative humidity (RH) in the box was increased by evaporating water from a beaker or decreased by insertion of a desiccant material and by flow of dry N_2 gas. Since it is rather difficult to fix the RH at a given value (except at the ambient RH, which is ~40% in our laboratory), we let the RH drift from an initial low value, e.g., 10%, by introducing a beaker of water at different temperatures. Usually this drift is slow, on the order of several hours from initial to final value. Each imaging experiment took about 1 min and this corresponds to a single RH value. This value was measured by an Omega RH-20C hygrometer. During drying experiments, the process was reversed, i.e., after reading a high RH, P_2O_5 pellets were introduced and the RH decreased slowly to a low final value of ~20%. Values below 20% were obtained by a combination of water absorption by P_2O_5 and dry N_2 flow.

3. Results and comments

3.1. Origin of contrast in SPFM: frequency dependence

For a sample of uniform composition, the contrast in SPFM is largely due to topographic variations across the scanned area. For an heterogeneous surface, local variations of the polarizability or dielectric constant ε contribute also to the contrast. As discussed previously [2], the spatial variation of ε can be dominating over that of the topography. For example, if two areas of the surface at the same topographic level have dielectric constants of 7 (mica, for example) and ∞ (a conductive region or a region of very high ε), the image can show a height difference of ~100 Å, depending on the force set point and tip distance.

The polarization force due to AC voltages was found to depend strongly on the frequency f, particularly at very low frequencies. A decrease of about one order of magnitude occurred when f increased above a certain cut-off value f_c. This dependence was measured by using an AC voltage of 10 V amplitude at a tip–surface separation of ~1000 Å. An example is shown in the inset of Fig. 2. The value of f_c depends strongly on the humidity, varying from several tens of mHz at ~10% RH to 1 Hz when RH is 20%. This range of RH values corresponds to the formation of the phase I water layer to be described below. At higher humidities, during the growth of a new phase (phase II), also to be described below, f_c varies from 1 Hz when RH is 20% to 20 Hz when RH is ~40%, at which point phase II is completed. Additional water adsorption continues to shift f_c up to 1 kHz when RH reaches 99%. The shift in f_c versus RH is fast at the beginning but tends to saturate at high humidities, as shown in Fig. 2. The small values of f_c indicate the operation of

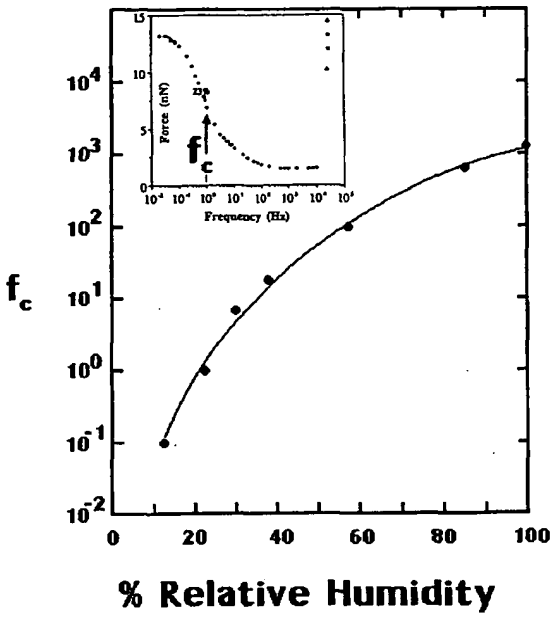

Fig. 2. Shift of the low frequency cut-off f_c of the polarization force versus relative humidity (RH). The tip was placed at a height of ~1000 Å above the surface and biased by an AC voltage whose frequency could be varied. An example of the variation of the polarization force with frequency for a fixed RH of 23% is shown in the inset. The spike at 27 kHz is due to the excitation of the mechanical resonance of the cantilever.

very slow processes, most likely involving transport of ions over the surface. These ions, presumably K^+ exposed by the cleavage of mica, become hydrated when the RH increases, which increases their mobility at the surface.

Imaging at a fixed polarization force was done most often using a ±2–3 V DC bias and slow scanning speeds, to take advantage of the higher signal at low frequency. For neutral surfaces, the image did not depend on the sign of V. Imaging using AC bias was also performed. In that case, we monitored either the AC response of the lever oscillation, using a lock-in amplifier, or its average (rms) DC deflection. This last method was necessary when the AC driving frequency was above half the mechanical resonance frequency of the cantilever, ~27 kHz. Unless otherwise indicated, the images shown in the next sections correspond to neutral surfaces and were obtained in the DC mode.

3.2. Low humidity phase

To study the condensation of water, we imaged freshly cleaved mica when exposed to increasing levels of relative humidity. After cleavage at RH < 20%, the images revealed a featureless surface with a roughness that is below the noise level of the measurement, which is ~0.5–1 Å, as shown in Fig. 3a. In spite of this lack of contrast, water is present on the surface, as we shall see below, even at humidities as low as ⩽5%, the lowest we have explored. The lack of contrast indicates that the water layer is uniform within the best lateral resolution currently achieved with our technique (~200 Å). This phase of water will be called phase I.

The uniformity of the water layer formed in these conditions could be artificially broken to create structures, i.e., contrast, by locally removing water with the AFM tip. In these experiments, the tip was brought into contact with the surface for a short time. The load applied during this contact is < 10 nN for a tip radius of ~500 Å, which is well below the inelastic threshold of mica [15]. After contact, the surface was imaged again in non-contact polarization mode. An example of these experiments is shown in Fig. 3. A circular hole is visible in Fig. 3b, with a diameter of ~2 μm centered around the contact point. The diameter of the hole increases with contact time, but the apparent depth at the center (50–100 Å) is independent of this parameter. We believe that the hole is due to the depletion of water in the layer around the contact zone [16]. The value of the apparent depth is easily explained by considering the difference of dielectric constants between the dryer area in the hole and the wet region surrounding it. The polarization force (at low frequency) in the area covered by water is about one order of magnitude larger than on dry mica (as expected from dielectric constant values of $\varepsilon_{\text{dry mica}} = 7$ and $\varepsilon_{\text{water film}} > 100$). To maintain a constant force, the feedback control displaces the sample by ~60 Å towards the tip when it scans over the dry patch. If the image is taken with an AC-biased tip at high frequency (1 MHz in Fig. 3c), the contrast disappears since the dielectric constants of the dry and wet regions become similar and the image

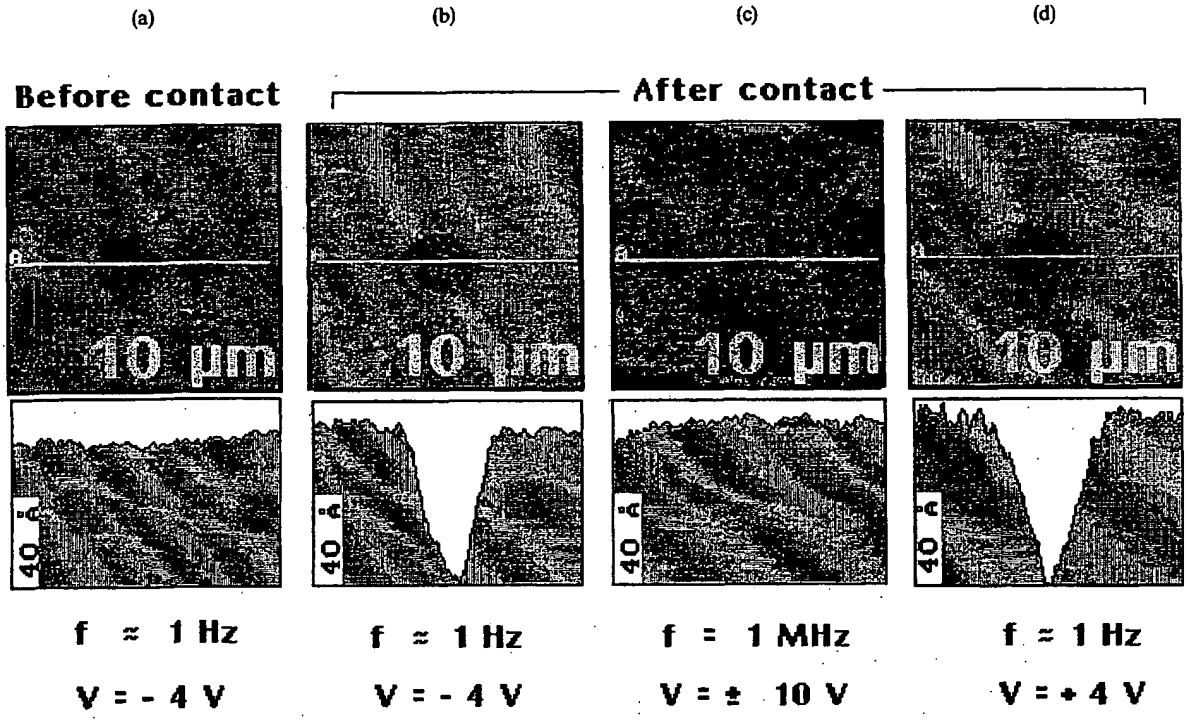

Fig. 3. SPFM images of mica exposed to a low humidity environment, ~5% RH. (a) No contrast is observed. (b) Contrast is observed after contact of the surface by the tip for a few milliseconds at a load of <10 nN. This removes water from the surface in the area surrounding the contact. The hole has an apparent depth of ~60 Å, a result of the different dielectric constants in dry hole and wet surroundings. (c) The apparent depth is below the noise level when using an AC bias of 1 MHz, and (d) returns to the original ~60 Å after returning to DC biasing.

appears flat within the noise level, as shown in Fig. 3c. The circular shape of these holes suggests that phase I is fluid in nature.

The equilibrium concentration of water at a given humidity is established very rapidly when the mica surface is clean, which is the situation found immediately after cleavage. After exposure to the ambient, however, it takes some finite time to establish equilibrium. For example, after locally removing water by contact with the tip, refilling of the hole by water may require several minutes when the RH<15%. At 15–20% RH, however, the hole fills fast enough to be unobservable. Similar phenomena were obtained for the next structure (phase II) at higher humidities. We believe that the kinetics of condensation is slowed down by an invisible layer of weakly bound contaminants.

3.3. Intermediate humidity phase

3.3.1. Growth

When the relative humidity increases above 20–25%, water condensation continues with the formation of 2D domains that grow as the humidity increases, as shown in Fig. 4. These domains correspond to the bright areas in the images, which expand as the humidity increases until they cover the entire surface when the RH reaches ~40%. This corresponds to a new phase which we shall call phase II. For easier visualization, the gray scale in these images is chosen so that dark corresponds to the initial phase I and bright to the new phase II regions. The apparent topographic height of these bright regions, however, is *lower* by ~2 Å than the surrounding dark regions. This topographic height difference indicates that the

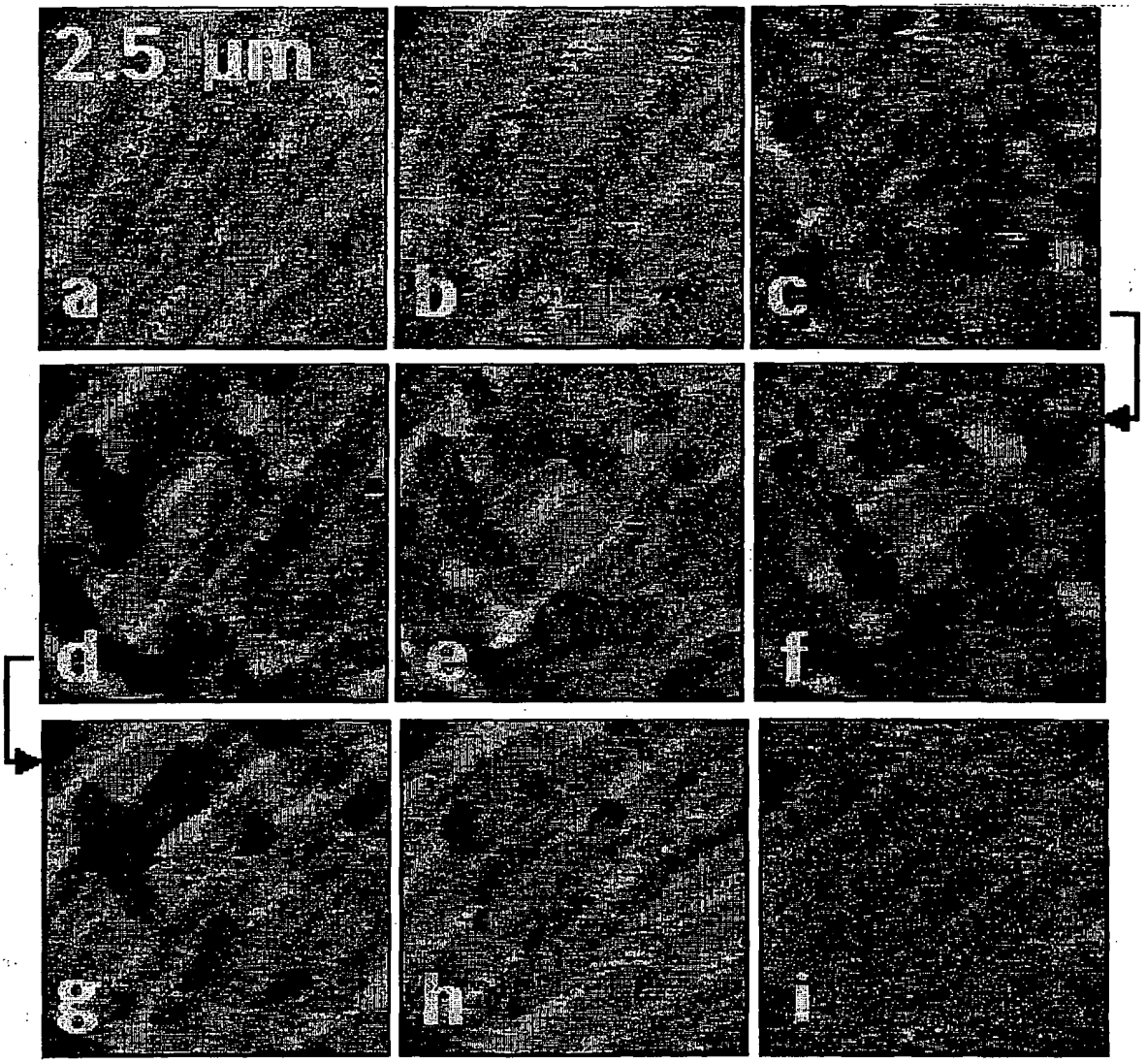

Fig. 4. Growth of a phase II water film with increasing humidity (figures at the bottom right corner of each image) above 20% is illustrated in these $2.5 \times 2.5\ \mu m^2$ SPFM images. The growth proceeds by the 2D increase in size of new domains (bright areas). The contrast between bright (phase II) and dark regions (phase I) is ~ 2 Å, with the bright regions lower than the dark ones. The domains of phase II cover completely the surface at $\sim 40\%$ RH.

dielectric constant is smaller in the new phase II than in phase I. The 2 Å difference would correspond to ~ 25 pN difference in the polarization force between the two phases if the tip were kept at the same height, which is small compared to the total attractive force of ~ 10 nN.

Unlike phase I, which shows a strong contrast change between low and high frequencies, the 2 Å height difference between phase I and II is maintained (within a factor of 2) up to frequencies of 1 MHz, the highest we could reach with our current instrumentation.

Phase II can also form with little or no noticeable change in image contrast, indicating that in this case the islands of phase II have dimensions below our lateral resolution limit of 200–500 Å. The adsorption of water can still be indirectly detected by the shift in the low frequency cut-off, as described above. It can also be detected by locally perturbing the surface with the tip at any stage during the adsorption. If the tip contact is done above 20% RH, a flat 2 Å high protrusion is created, as shown in Fig. 5c, indicating that phase II is replaced by phase I in the area of contact (this is the only image in this paper where the gray scale is such that phase I appears brighter than phase II).

The reason why large islands of phase II form in some cases, while no contrast is observed in others, is not yet completely understood. It is possibly related to the incomplete control in the present experiments of two important parameters: substrate temperature and contamination. Temperature might determine, for example, whether direct evaporation and condensation is dominant over surface diffusion, as we will see in the evaporation experiments described below. The competition between these two processes, coupled

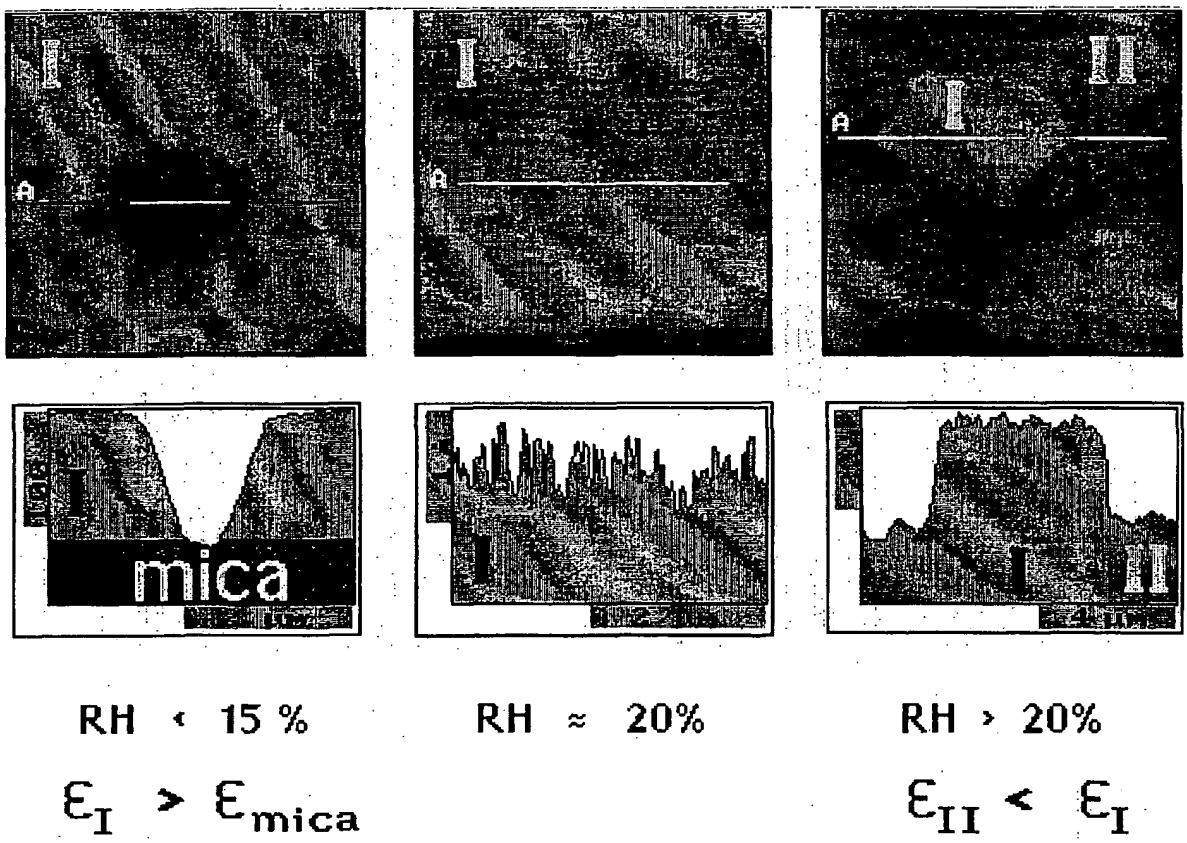

Fig. 5. Contrast in SPFM is determined by the local polarizability (dielectric constant) as much as by topography. This is illustrated in these images. (a) Phase I film at a RH of <15%. The hole was created by contacting the tip with the mica for a short time (a few milliseconds). This removed water, producing a drier region around the contact with an apparent depth of ~100 Å. This value is due to the different dielectric properties of wet and dry mica. The hole fills up again with water with exposure. At RH≈20%, the hole fills too fast to be observed. (b) At RH>20%, phase II forms. Contact with the tip again removes water locally exposing a hole that is covered with phase I water. Phase I appears higher than phase II by ~2 Å, as shown in (c).

with variations in the density of nucleation centers (that might be influenced by contamination), could determine whether growth is uniform, with many small islands, or proceeds by growth of fewer and larger islands, as in the case of Fig. 4.

3.3.2. Structure of phase II

There are other remarkable points about phase II besides its lower dielectric constant relative to phase I. One is the shape and orientation of its boundaries with phase I. These tend to be

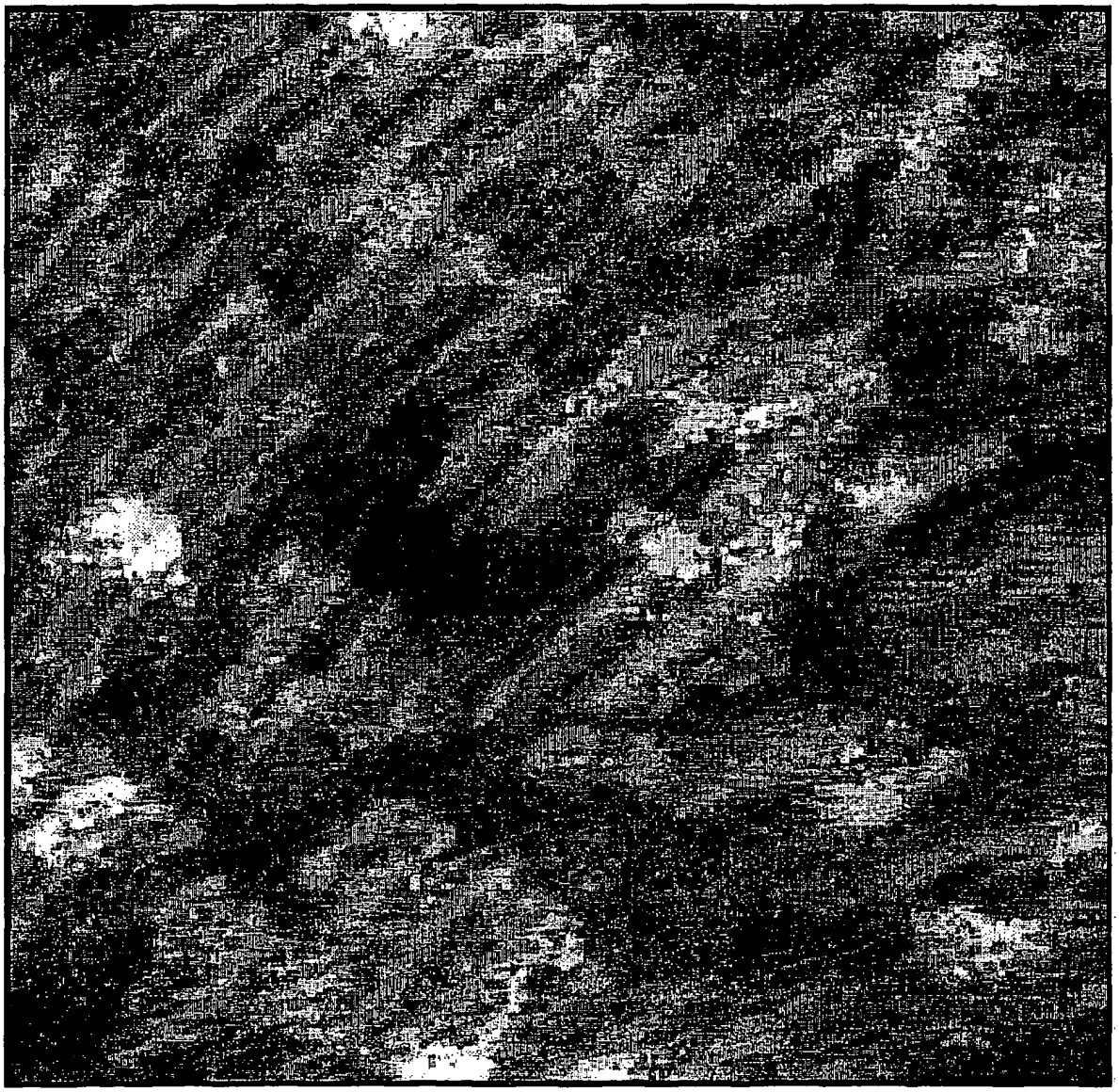

Fig. 6. Large SPFM image showing a film of phase II water (bright regions) partially covering the surface at 35% RH. Notice the polygonal shape of many of the boundaries lines between the two phases.

straight, with angles of 60 and 120° between adjacent boundary lines. This can be seen when large islands are formed like those shown in Fig. 6 and more clearly in Fig. 7. This observation seems to indicate a crystalline structure for water in phase II.

The epitaxial relationship between the mica lattice and phase II was investigated by contact mode imaging (the standard AFM operation mode) after obtaining the non-contact images. This allowed us to obtain lattice resolved images of the mica substrate and to measure its orientation relative to that of the polygonal domains of phase II, as shown in Fig. 8. A histogram of measurements of the relative angles is shown in Fig. 9. As can be seen, there is a clear preferential orientation of the domain edges along the principal unit cell directions of mica at 0, 60 and 120°. The scattering in the data is in part due to the round appearance of some domains boundaries due to our limited in plane resolution.

3.4. Drying of water layers

The reverse process of drying was also investigated. This was performed in several ways. One was simply by decreasing the RH in the chamber. Another was to warm the surface while keeping the RH constant. A third method consisted in using the tip to remove water, by bringing it into physical contact with the surface as already shown in the previous section.

In the first drying method, the humidity content of the chamber was lowered by the introduction of a desiccant material. An example of the images taken during this drying process is shown in Fig. 10. As the humidity decreases, numerous holes form inside the areas covered by phase II as a

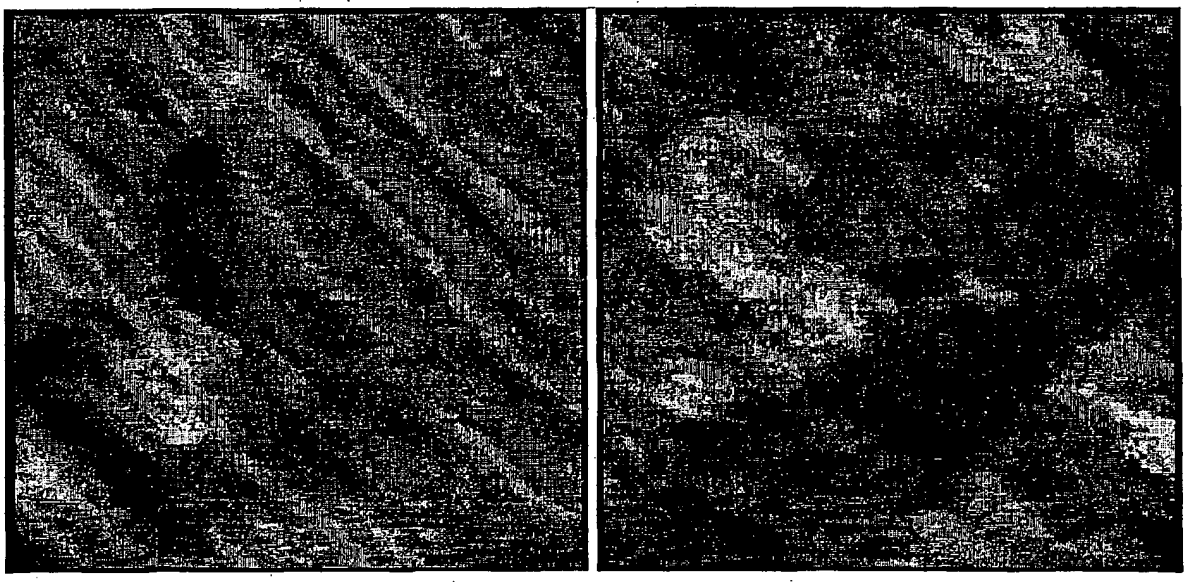

Fig. 7. Details of the boundary between phase I and II showing straight lines making angles of 60 and 120°, indicating the hexagonal shape of the domains.

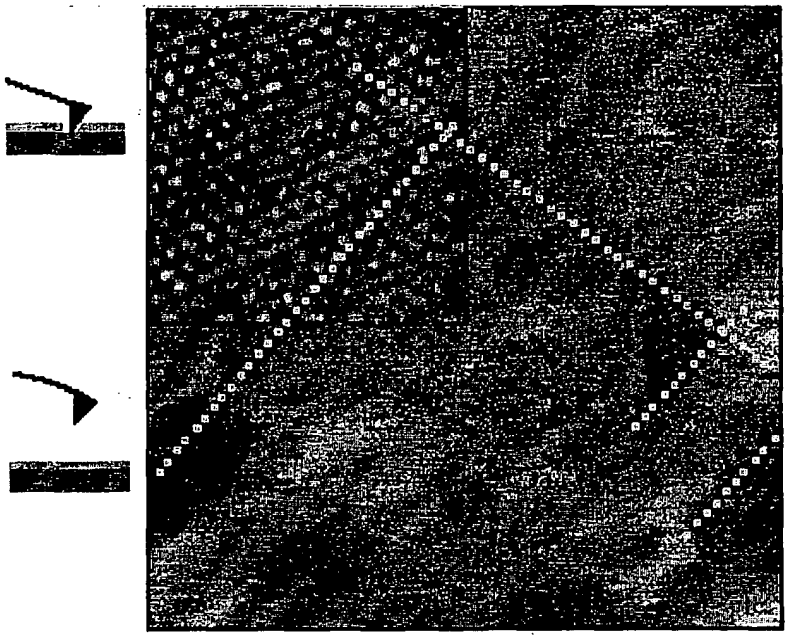

Fig. 8. Measurement of the relative angles between phase II domain boundaries and mica crystallographic directions is illustrated in this composite image: a SPFM image showing mica partially covered with phase II water (bright areas) is acquired first. Immediately afterwards, the AFM tip is brought into contact with mica and a standard lattice resolved image is obtained (inset). This allows us to easily measure the relative orientations.

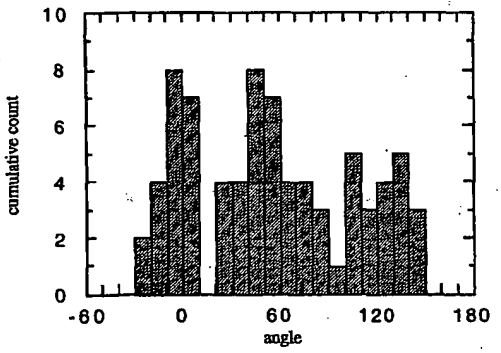

Fig. 9. Histogram of measured angles between phase II boundary directions and the main crystallographic directions of the mica basal plane. A clear angular epitaxial relationship is observed with peaks at 0, 60 and 120°.

function of time. At the same time, small regions of phase II nucleate inside the dark areas of phase I. The total area covered by phase II, however, decreases with time until the surface is completely covered by phase I, at 21% RH in that experiment. This drying behaviour seems to indicate that direct evaporation and adsorption from the gas phase is dominant over surface diffusion. The details of the drying process depend also on the previous exposure of the surface to air, indicating that impurities adsorbed from the gas phase may play an important role by providing nucleation sites.

In the second method of drying, we allowed the substrate to warm up, while maintaining the RH constant. This warming occurred first accidentally when radiation from the laser beam reflecting off the back of the cantilever illuminated the sample as well, as a result of imperfect focusing and high laser power. Optimization of the focusing and operation of the laser at sufficiently low power are clearly important conditions in these experiments. For the present case, we then purposely allowed the sample to warm up by using sufficiently high laser power. Unfortunately, however, we could not measure the local temperature of the mica under the tip.

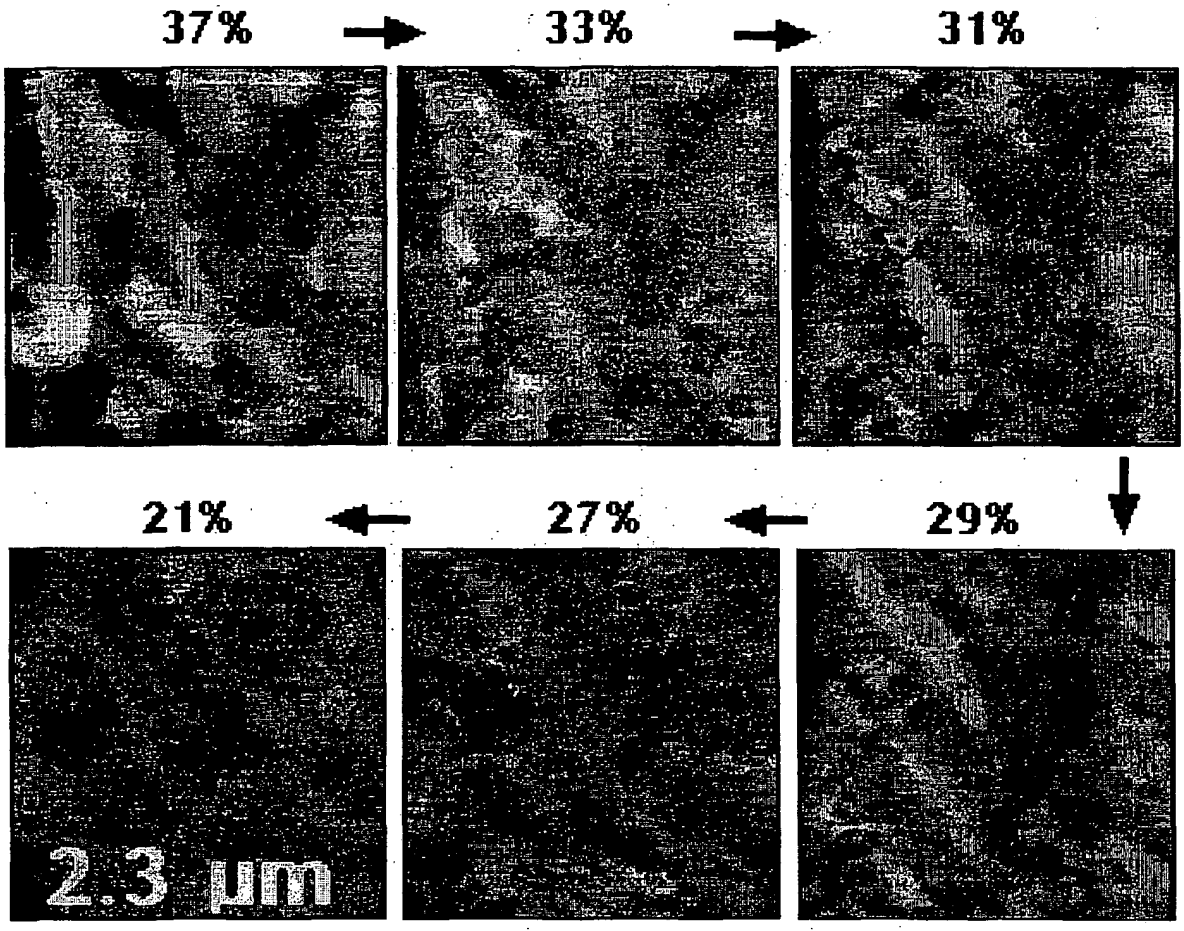

Fig. 10. Drying of phase II water from the mica surface as a function of decreasing humidity at approximately constant room temperature. Drying proceeds by formation of numerous holes inside the domains of phase II, rather than by shrinkage of the domains through recession of domain boundaries.

In this manner, we could observe the drying process while the RH was kept at 40%. An example is shown in the series of $10 \times 10\ \mu m^2$ images of Fig. 11. As can be seen, the disappearance of phase II occurs by continuous recession of its boundaries. This result can be interpreted in two ways. One is that surface diffusion is fast enough to heal any hole left by the evaporation of water to the gas phase and also to prevent the nucleation of small phase II islands inside the areas covered by phase I. Another interpretation is that phase II is "melting" and converting to phase I which might exist on the surface at higher humidities above room temperature. It is not known with the present data which of these interpretations is correct.

3.5. *High humidity case ($\geq$40%)*

3.5.1. *Hydrophilic mica*

After completion of phase II, if the RH increases above 40%, water continues to adsorb on the mica substrate. The SPFM images, however, did not reveal any contrast change even for humidities as high as 99%. The only indication that water is condensing on the surface is the continuous shift of the low frequency cut-off f_c discussed above,

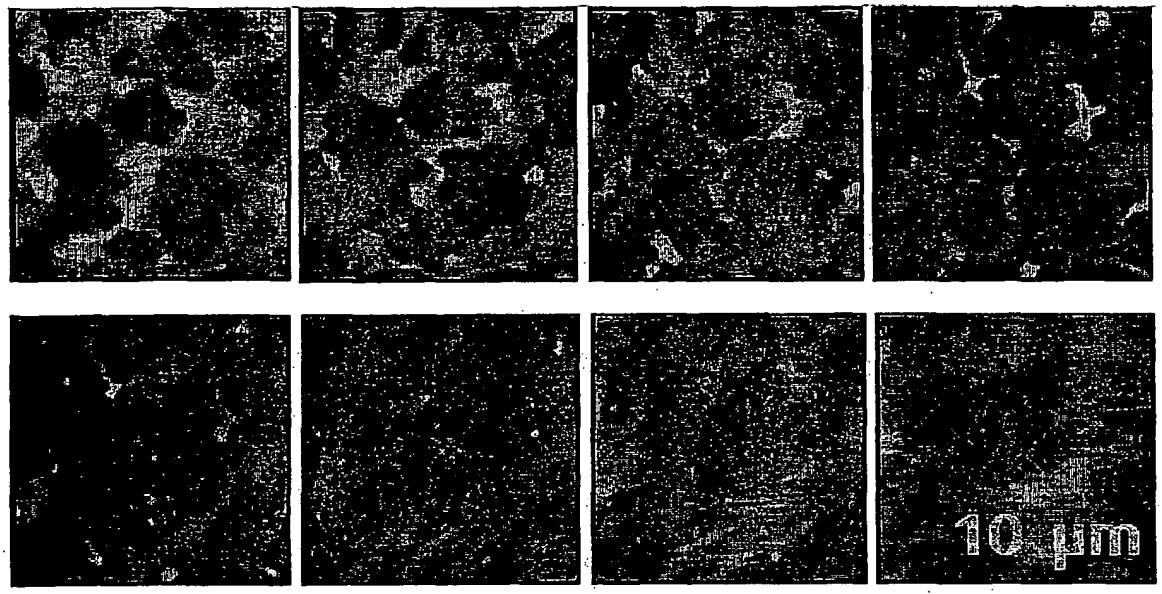

Fig. 11. Drying of phase II water at constant humidity (40%), induced by heating. Heating was produced by using high power and defocused conditions of the laser beam illuminating the back side of the cantilever which is used to measure its deflection. The temperature is unknown. Under these conditions, phase II disappears by recession of its boundaries with phase I.

which reached a value of 1 kHz at 99% RH. This result indicates that above phase II, the layers of water are very mobile, as expected from a liquid film wetting a hydrophilic surface. To observe thick water structures (multilayers) we had to resort to a perturbation of the surface to restrict the mobility of the liquid water, as explained in the following section.

3.5.2. Hydrophobic mica

It is known that after long exposure to air, mica becomes slightly hydrophobic. This occurs possibly by the accumulation of contaminant material of organic origin. Sometimes contaminant material can be imaged by contact AFM at very low loads under liquid, as we have shown recently [16]. Imaging mica that has been exposed to ambient air for several hours in the SPFM mode did not reveal the formation of any surface structure even at a RH of 99%. However, water could be forced into the surface by contact with the tip at high humidities. An example of such an experiment is shown in Fig. 12a. The image shows a water droplet with an apparent height of 50 Å which was produced by such a contact. The explanation of this experiment is as follows: a capillary neck of water forms around the contact region from vapor condensation, due to the negative Kelvin radius that lowers the saturation value of the vapor pressure. In addition, the tip might displace locally some of the contaminants. Upon retraction of the tip, a droplet is left on the surface with a finite contact angle with the hydrophobic surface. By assuming a spherical cap shape for the droplet, a rough estimate for the contact angle of $\sim 5°$ could be obtained from its height and base diameter. Precise values of the contact angle cannot be obtained at this stage since the measured apparent height is determined by a combination of both topography and dielectric constant. The droplets were found to disappear by evaporation unless the humidity was kept at or above 56%. It is possible also that the droplet is stabilized by some dissolved impurities from the tip.

We used droplets produced by this method to determine the effect of the forces of interaction with the tip. We could observe the displacement of droplets when the pulling force due to the

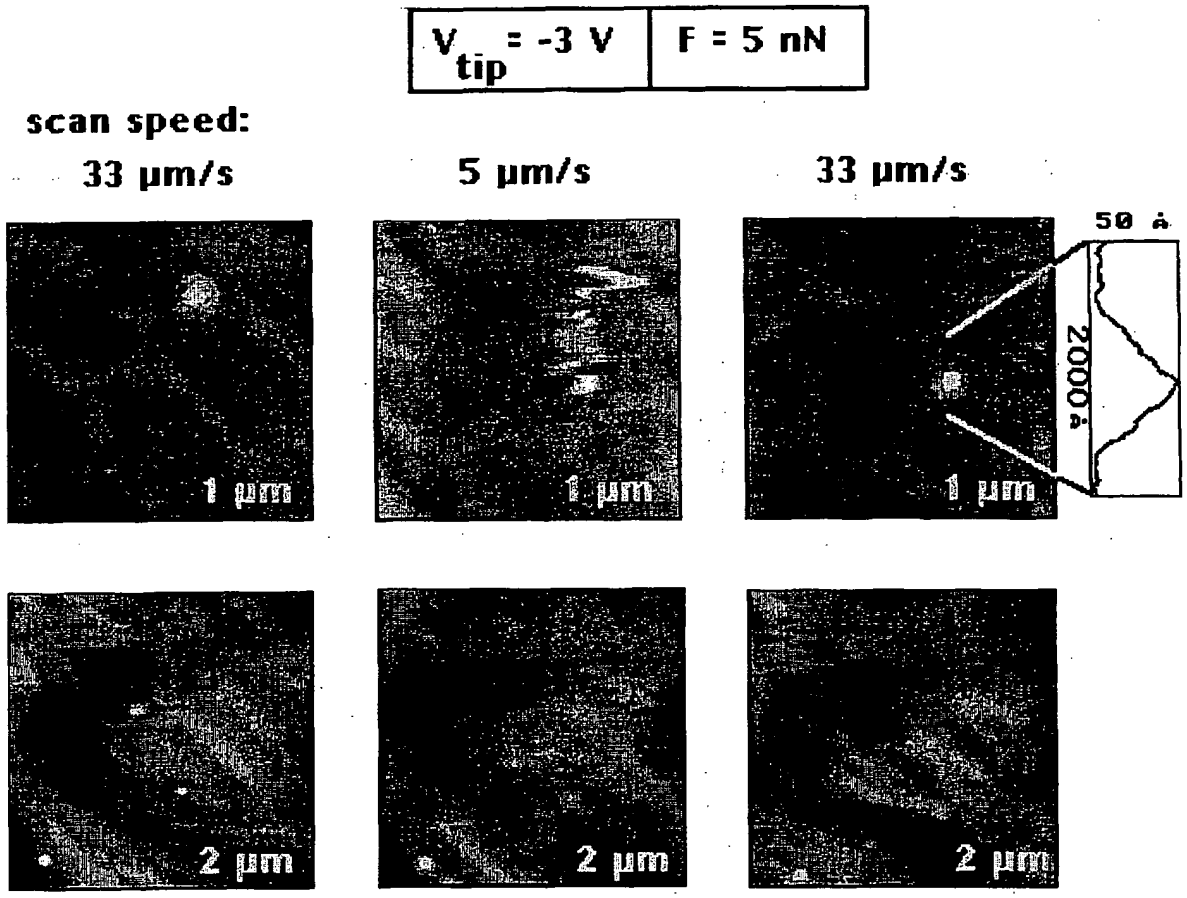

Fig. 12. $1 \times 1\ \mu m^2$ SPFM images showing a droplet of water (top left image) deposited on hydrophobic mica at 56% RH. Mica became hydrophobic after several hours exposure to the air. The droplet was produced by forcing the tip into contact with the surface at high humidity (99%). The center image shows the displacement of the droplet by the tip by increasing the attractive force. This is done here by scanning slowly (speed decreased from 33 to 5 μm/s), which was sufficient to cause dragging along the slow scan direction (vertical). The bottom images show three $2 \times 2\ \mu m^2$ snapshots of the process of alignment of three droplets using the same procedure.

electrostatic interaction was large enough. This is shown in Fig. 12b, where the droplet was moved by decreasing the scanning speed from 33 to 5 μm/s (in the x direction). The droplet is dragged by the tip along the slow scanning direction (y). By controlling the force through the applied bias and/or the scanning speed, nanodroplets of water could be manipulated, as shown in the example of the three bottom images in Fig. 12. Three droplets produced by tip contact with the hydrophobic mica are aligned by the displacement process described. A more detailed account of the formation and manipulation of droplets will be published soon [17].

4. Discussion

The dielectric properties of mica and other layered aluminosilicates, such as clays and montmorillonites have been the subject of research in the past [18]. The large enhancement of the dielectric constant at low frequencies has been documented in these earlier works and the role of water hydrat-

ing ions has been pointed out. Values of ε as high as several thousand have been reported and have been associated with the formation of these mobile hydrated ions [19,20]. It is not surprising, then, that the contribution of the surface of materials to the dielectric constant at very low frequencies can be very large. Ions may be present at the surface as a result of the substrate lattice structure or from contamination. This is relevant for SPFM since it is the surface dielectric properties that largely determine the polarization force, particularly at low frequencies.

Muscovite mica cleaves through the alkali containing planes, K^+ in this case. These planes separate negatively charged aluminosilicate groups that expose a honeycomb array of oxygen atoms. The 5.2 Å periodicity of this oxygen array is what is imaged in contact mode AFM. Ideally half the K^+ ions should remain in each of the two cleavage planes, although frequently, small imbalances in their distribution result in charged surfaces. Solvation of water around K^+ ions in Ni(110) has been observed using IR and HREELS [21,22]. It has also been observed in the case of clay minerals [8]. The continuous shift of f_c with humidity is probably related to the increased mobility of these hydrated ions as the amount of adsorbed water continues to increase. The hydrated ions are not restricted to the first monolayer and probably distributed themselves in a few water layers at high humidities like the counterions in the electrochemical double layer.

At humidities between 20 and 40%, it is the average dielectric constant of the surface (from phase I and phase II areas) that is measured in the experiments described is Section 3.1. The small local variations due to the two dielectrically different phases give rise only to a small contrast change. The lower value of ε in phase II could be due to a smaller mobility of the hydrated ions in areas covered by that phase. The persistence of the contrast difference between the two phases up to 1 MHz, however, seems to indicate that other contributions in addition to mobile ions are important. For example, there could be a reduction of the dipolar contribution of water molecules in phase II if we assume that this phase is crystalline, due to the orientation restriction imposed by the crystal structure. In fact, one would expect a reduction of ε in phase II relative to solid ice. This is due to the formation of hydrogen bonds between the water molecules and the mica and by the reduced spatial conformation imposed by the 2D nature of the film relative to the 3D ice case, which makes more difficult the formation of Bjerrum defects [23].

There is a substantial amount of literature on water adsorption on many surfaces and on mica, in particular, that has a bearing on the present study. The formation of epitaxial ice films on muscovite mica was used to determine the slip directions and partial dislocations of mica [24]. The angular epitaxial relationship found in our study for phase II (Section 3.3.2), favors the idea this phase is indeed solid. The observed directions of the angular epitaxial relationship (at 0, 60 and 120°) indicate that it takes place along the closed packed directions. Since the ice periodicity in the (0001) plane is 4.5 Å, either a moiré-type coincidence takes place every ~9 mica unit cells or perhaps there is a distortion (flattening) of the O ring structure in the monolayer that would increase the hexagon size to conform with the mica lattice. Because of our limited resolution in the *xy*-plane, no molecular scale details of the structure of this layer could be obtained.

The adsorption of water on mica at room temperature (18°C) has been studied by Beaglehole and Christenson [25] using ellipsometry. They found that the average thickness of the water layer increases with relative humidity, reaching ~2 Å at RH ≈ 50%. This could correspond to the completion of phase II at ~40–50% RH and indicates the formation of one complete monolayer of water. The ellipsometry experiment however, did not provide information on the solid or liquid character of the monolayer water film.

We could not observe contrast when the clean mica surface was exposed to high humidities (>50%), although we know from the continuous shift of the low frequency cut-off that water is adsorbing on the surface. We believe that this is due to the fact that water in excess of a monolayer is liquid and thus very mobile, preventing the observation of contrast in the images. The ellipsometry experiments cited above indicate that, at

high humidities, the thickness of the film increases up to ~20 Å near saturation. If the films produced in our case are of similar limited thickness at the highest humidities studied, it would explain the observed saturation of the frequency cut-off at ~1 kHz.

Christenson and Israelachvili [26] describe experiments where crystalline deposits can form on mica as a result of water adsorption. According to these authors, the deposits are due to formation of K salts formed upon drying of the water films. Since the contrast in our SPFM images is largely due to the mobility of solvated ions, it is clear that they are present and mobile in both phases I and II. However, phase II disappears upon drying, leaving no solid residues on the surface. This rules out the possibility of phase II being made by solid salt precipitates.

The properties of thin water films at temperatures below the freezing point have been studied in detail by Dash and coworkers over the last few years. Of particular relevance to the present work is their recent report about the formation of a monolayer of solid ice before the formation of *liquid* multilayers at high humidities [27] in the temperature range of −30 to 0°C. The solid or liquid nature of the film formed was inferred from the measured value of the dielectric constant, which is lower for ice than for water at frequencies >10 MHz [18,28]. If phase II water is solid, as the present data tends to support, it would extend this finding to temperatures of up to 21°C. The formation of the fluid-like, lower density phase I, was not observed by these authors and thus appears to be characteristic of adsorption at temperatures >0°C.

The equilibrium between phase I and phase II is established by exchange of molecules which are transported through the gas (evaporation and condensation) and by surface diffusion. The relative importance of either of these two different mechanisms is likely determined by temperature. Unfortunately, the present experiments do not provide sufficient information to warrant a more detailed discussion on that subject. For that, the phase diagram of molecularly thin films of water on mica needs to be determined in more detail with the addition of temperature variation. We are currently developing a new system to accomplish this.

5. Summary and conclusions

We have shown that the application of the newly developed SPFM technique appears to be very powerful in the study the structure of liquid films and droplets condensing on solid surfaces. Water monolayers could be imaged as they condense and evaporate from the mica surface at or near room temperature. It is clear that several phases form depending on relative humidity. At low humidities (below ~20%), a phase forms that has a homogeneous 2D structure (within the present lateral resolution of the technique of 200–500 Å). It has the characteristics of a fluid phase (liquid or gas) in that its boundaries with dry patches are round. A second phase forms at higher humidities (above ~20%) that has the characteristics of a solid phase with hexagonal symmetry, perhaps corresponding to an ice layer, as proposed by other authors. This solid phase covers completely the surface when the RH reaches 40–50%. Above that value, condensation produces a thicker liquid film as evidenced by the continuous shift in the low frequency cut-off, and by the observation of formation of droplets when the mica is contaminated by air exposure.

Acknowledgements

This work was supported by the Director, Office of Energy Research, Basic Energy Sciences, Materials Sciences Division of the US Department of Energy under contract number DE-AC03-76SF00098. J.H. acknowledges a grant from the Academia Sinica and the Committee of Science and Technology of Shanghai (P.R. China).

References

[1] For a review, see the series of monographs, R. Wiesendanger and H.-J. Güntherodt, Eds., in: Scanning Tunneling Microscopy I, II and III, Vols. 20, 28 and 29 (Springer, Berlin, 1992/1993).

[2] J. Hu, X.-D. Xiao and M. Salmeron, Appl. Phys. Lett. 67 (1995) 476.
[3] Q. Dai, J. Hu, A. Freedman, G.N. Robinson and M. Salmeron, J. Phys. Chem., in press.
[4] Q. Du, R. Superfine, E. Freysz and Y.R. Shen, Phys. Rev. Lett. 70 (1993) 2313.
[5] Q. Du, E. Freysz and Y.R. Shen, Phys. Rev. Lett. 72 (1994) 238.
[6] J. Porter and A.S. Zinn, J. Phys. Chem. 97 (1993) 1190; Phys. Rev. Lett. 73 (1994) 2879.
[7] M.F. Toney, J.N. Howard, J. Richer, G.L. Borges, J.G. Gordon, O.R. Melroy, D.G. Wiesler, D. Yee and L.B. Sorensen, Nature 368 (1994) 444.
[8] J. Glosli and M. Philpott, in: Proc. Symp. on Microscopic Models of Electrolyte Interfaces, Vols. 93–95 (Electrochemical Society, Pennington, 1993) p. 90; see also the references cited in Ref. [7].
[9] P.A. Thiel and T.E. Madey, Surf. Sci. Rep. 7 (1987) 211.
[10] R.M. Pashley and J.N. Israelachvili, J. Colloid Interface Sci. 101 (1984) 511.
[11] H.K. Christenson, J. Phys. Chem. 97 (1993) 12034.
[12] J. Hu, X.-D. Xiao, D.F. Ogletree and M. Salmeron, Science 268 (1995) 267.
[13] See, for example, J.D. Jackson, Classical Electrodynamics (Wiley, New York, 1975).
[14] We used a commercial RHK 100 control unit.
[15] J. Hu, X.-D. Xiao, D.F. Ogletree and M. Salmeron, Surf. Sci. 327 (1995) 358.
[16] A detailed account of this drying process by the AFM tip is being prepared for future publication.
[17] J. Hu and M. Salmeron, J. Vac. Sci. Technol., in press.
[18] G. Sposito and R. Prost, Chem. Rev. 82 (1982) 571.
[19] V. Mehrotra and E.P. Giannelis, J. Appl. Phys. 72 (1992) 1039.
[20] R. Raythatha and P.N. Sen, J. Colloid Interface Sci. 109 (1986) 301.
[21] N. Kizhakevariam, I. Villegas and M.J. Weaver, preprint.
[22] G. Pirug and H.P. Bonzel, preprint.
[23] N. Bjerrum, Science 115 (1952) 385.
[24] J.L. Caslavsky and K. Vedam, J. Appl. Phys. 42 (1971) 516.
[25] D. Beaglehole and H.K. Christenson, J. Phys. Chem. 96 (1992) 3395.
[26] H.K. Christenson and J.N. Israelachvili, J. Colloid Interface Sci. 117 (1987) 576.
[27] H. Fu and J.G. Dash, in: Proc. APS March Mtg., San Jose, CA, March 20–24, 1995, preprint.
[28] F. Bruni, G. Consolini and G. Careri, J. Chem. Phys. 99 (1993) 538.

Date: March 8, 2004

Appendix

Serial No.	Regular Application Filing Date	Status	Examiner/ Group Art Unit assigned (per PAIR or filing receipts)	Attorney Docket No.
1st Family				
09/477,997	January 5, 2000	Issued as patent (6,635,311) after examination by Examiner Fletcher	Fletcher III (1762)	083847-0110
10/449,685	Continuation of 477,997; filed June 2, 2003	Not yet examined	1762	083847-0217
2nd Family				
09/866,533	May 24, 2001	December 1 office action	Fletcher III (1762)	083847-0109
10/212,217	Continuation of 866,533 filed August 6, 2002	No examination; Set of interfering claims filed August 6, 2002; telephone call with Examiner on restriction requirement on Feb. 27, 2003	Fletcher III (1762)	083847-0139
10/301,843	Continuation of 866,533 filed November 22, 2002	No examination; Request for Interference Filed October 17, 2003; telephone call with Examiner about status of case in view of other cases	Fletcher III (1762)	083847-0140
3rd Application				
10/059,593	January 28, 2002	Not yet examined	Fletcher III (1762)	083847-0208

Date: October 27, 2003

Appendix

Serial No.	Regular Application Filing Date	Status	Examiner/ Group Art Unit assigned (per PAIR or filing receipts)	Attorney Docket No.
1st Family				
09/477,997	January 5, 2000	Issued as patent after examination by Examiner Fletcher	Fletcher III (1762)	083847-0110
10/449,685	Continuation of 477,997; filed June 2, 2003	Not yet examined	1762	083847-0217
2nd Family				
09/866,533 (PRESENT APPLICATION}	May 24, 2001	Restriction requirement; first Office action received December 4, 2003	Fletcher III (1762)	083847-0109
10/212,217	Continuation of 866,533 filed August 6, 2002	No examination; Set of interfering claims filed August 6, 2002	Fletcher III (1762)	083847-0139
10/301,843	Continuation of 866,533 filed November 22, 2002	No examination; Request for Interference Filed October 17, 2003	Fletcher III (1762)	083847-0140